Kinetics and Curing Mechanism of Epoxy and Boron Trifluoride Monoethyl Amine Complex System

YE-SHIU LI, MING-SHIU LI, FENG-CHIH CHANG

Department of Applied Chemistry, National Chiao Tung University, Hsinchu, 300, Taiwan, Republic of China

Received 18 January 1999; accepted 7 May 1999

ABSTRACT: The kinetics of cationic polymerization of epoxy resin has been studied. Due to multiple reaction exotherms and irregular baselines involved in this system, the ASTM E 698 method was chosen to determine the kinetic parameters of this epoxy/BF_3-MEA system. The DER 332/BF_3-MEA system follows the first order active chain end (ACE) reaction mechanism. The adding of the hydroxyl group into the system is prone to decrease the activation energy and shifts the curing into the activated monomer (AM) mechanism due to the stronger nucleophilicity of the hydroxyl group than the epoxide group. On the other hand, the DER 331/BF_3-MEA system possesses lower activation energy because the DER 331 contains more hydroxyl groups—α-glycol and secondary alcohol. The former is the major contributor in lowering the activation energy. The hydroxyl group also can act as a chain transfer agent by retarding the propagation process, thus the reaction rate of the DER 332/BF_3-MEA system is higher than the DER 331/BF_3-MEA system. The DER 332/BF_3-MEA system shows good correlation between the experimental data (FT-IR, DSC, and GPC) and the simulation curve based on ASTM E 698 before gelation, while a larger deviation is observed in the DER 331/BF_3-MEA system. After gelation, the hydroxyl group also acts as an active site to react with residual epoxy monomers and obtain a more condense matrix. © 1999 John Wiley & Sons, Inc. J Polym Sci A: Polym Chem 37: 3614–3624, 1999

Keywords: epoxy; cationic polymerization; kinetics; reaction mechanism

INTRODUCTION

Generally the curing reaction of epoxy resin follows the nth order reaction or the autocatalytic reaction. The curing mechanism of the epoxy/amine system follows the autocatalytic model due to the increasing concentration of the hydroxyl group during the curing reaction that accelerates the curing reaction.[1–7] Patel et al.[8] claimed that the first order reaction was in the epoxy/diethyltriamine system, however, his reported data was inconsistent. Woo and Seferis[9] reported that the epoxy/trimellitic anhydride system follows the second order kinetic model because the ester group instead of the hydroxyl group appears during the curing reaction. Similar results can also be obtained in the epoxy/imidazole system. Heise and Martin[10] reported that the epoxy/2-ethyl-4-methyl-imidazole system follows the first order kinetic model. Ghaemy[11] reported that the cationic polymerization of epoxy/BF_3-EDA (boron trifluoride ethylene diamine) system follows the first order reaction by forming the epoxy-cationic complex and the reaction order becomes 1.45 at the propagation process (or etherification). The BF_3-EDA content of 6–10 phr was employed in this study, which is substantially higher than normal usage of 2 phr. Thus, the polymerization process is accelerated by the presence of the amine group from the EDA.

The widely used differential scanning calorimetry (DSC) softwares have been used to analyze

Correspondence to: F.-C. Chang (E-mail: changfc@cc.nctu.edu.tw)

Journal of Polymer Science: Part A: Polymer Chemistry, Vol. 37, 3614–3624 (1999)
 CCC 0887-624X/99/183614-11

curing kinetics including isothermal, Borchardt and Daniels,[12] and American Society for Testing and Materials (ASTMVE) 698[13] methods. However, only the ASTM E 698 method can be applied to the cationic polymerization of epoxy resin because of multiple exotherms and irregular baseline. For the isothermal method, the reaction heat released from the higher temperature exothermic peak may not totally appear at a lower curing temperature. Thus the isothermal method suffers from the difficulty in determining the true reaction heat. The Borchardt and Daniels method is also inapplicable in this cationic polymerization of epoxy resin because the occurrence of the overlapping reaction peaks in addition to the decomposition reaction during curing. Therefore, the ASTM E 698 method has been adopted to analyze the curing kinetics in this study.

Two commercially available DGEBA type epoxy resins, DER 331 and DER 332, are employed in the study. The DER 331 resin contains substantially more hydroxyl groups than that of DER 332. The effect of hydroxyl group on epoxy curing mechanism and kinetics will be discussed later.

EXPERIMENTAL

Materials

Two DGEBA type epoxy resins, DER 331 and DER 332, with epoxide equivalent weights of 190 and 170, were purchased from the Dow Chemical Company (Midland, Michigan, USA). The compositions of these two epoxy resins are listed in Table I. The boron trifluoride monoethyl amine complex (BF_3-MEA) was supplied by the Lancaster Synthesis Ltd, Lancashire, UK. The ethylene glycol was obtained from the Union Chemical Works Ltd. of Hsinchu, Taiwan. The 3-phenoxy-1,2-propanediol was supplied by the Aldrich Chemical Company of Dorset, UK. The 1-phenoxy-2-propanol was supplied by the Lancaster Synthesis Ltd.

Procedures and Instrumentations

In order to mix completely the solid BF_3-MEA and the epoxy resin, the epoxy resin is heated to 120°C. Then, 2 phr BF_3-MEA is added and dissolved in the resin. Then the solution is cooled down to room temperature by immersing the solution in a cold water bath. Since the decomposition temperature of the BF_3-MEA is above 85°C,[14] the polymerization of epoxy is insignificant below this temperature. Thus the extent of reaction is ignored during the dissolving procedure. Calculated amount of the hydroxyl-containing compound (3-phenoxy-1,2-propanediol, 1-phenoxy-2-propanol, ethylene glycol or phenol) is added and mixed completely at room temperature.

The kinetic studies and T_g measurements are conducted by a TA Instruments DSC 910 (New Castle, Delaware, USA) with heating rates of 2.5, 5, 10, and 20°C/min from 50–300°C. The decomposition profile of the system is conducted by a TA Instruments TGA 951 with a constant heating rate of 10°C/min under air purging. The molecular weight measurement is carried out by using a Waters 410 GPC (Milford, Massachusetts, USA) using flow rate of 1 ml/min. A Nicolet AVATAR 320 FT-IR (Madison, Wisconsin, USA) is used to analyze the epoxide group of the system with a resolution of 2 cm^{-1}.

Table I. The Compositions of Epoxy Used in This Study

	Materials	
Items/Unit	DER 332	DER 331
Viscosity (cps)[a]	4,805	11,623
EEW (g/mol)[a]	173.4	185.6
DGEBA [n = 0] (%)[b]	98.0	79.3
[n = 1] (%)	0.0	11.1
[n = 2] (%)	0.0	2.2
α-Glycol (%)	—	7.7
Others (%)	2.0	—
Water, max (ppm)[a]	253.0	570.0
Hydro. Cl,[c] max (ppm)[a]	201.0	234.0

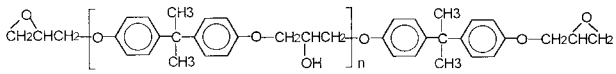

Bisphenol-A based epoxy resin

[a] Represents the data observed from the certificate of analysis supplied by the Dow Chemical Company.

[b] Percent represents the area fraction of optical density measured by the refractometer of GPC.

[c] Hydro. Cl (hydrolyzable chloride) represents the 1,2-chlorohydrin; its chemical structure is illustrated as follows

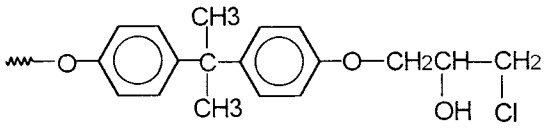

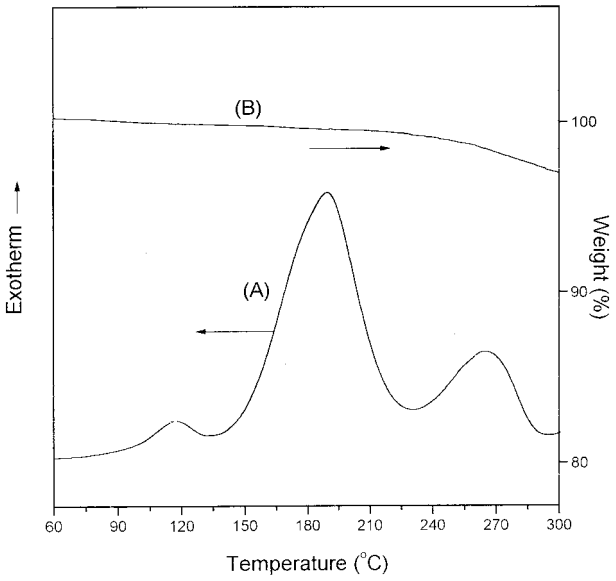

Figure 1. DSC thermogram (A) and TGA degradation curve (B) of DER 331/BF_3-MEA system at a heating rate of 10°C/min.

RESULTS AND DISCUSSION

Active Chain End (ACE) Mechanism

Penczek et al.[15,16] proposed that the cationic polymerization of DER 332/BF_3-MEA system follows the ACE mechanism as shown below:

ACE Initiation

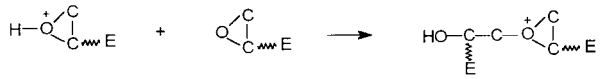

ACE Propagation

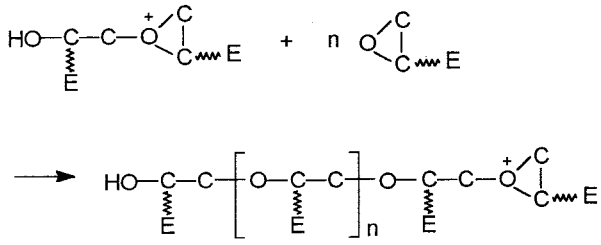

The active monomer is created by the BF_3-MEA, and the concentration of the active monomer is considered to be constant because a constant BF_3-MEA concentration is employed. Therefore, the reaction rate is a first order to the concentration of the epoxy monomer.

ASTM E 698 Method

Figure 1(A) shows the DSC thermogram of the epoxy (DER 331) cured by the BF_3-MEA, a small exotherm appears at about 120°C, followed by a larger exotherm between 130 and 220°C. This small exotherm at 120°C can be attributed to the thermal conversion of BF_3-MEA to HBF_4 that has been previously reported.[17,18] This larger exotherm is caused by the etherification reaction of the oxirane initiated by the HBF_4 complex. The explanation of the final exotherm at 260°C is somewhat controversial. Chen and Pearce[19] explained this peak as result of further curing, while Tackie and Martin[14] interpreted it as the reaction between hydroxyl and oxirane. Figure 1(B) shows the corresponding dynamic TGA scan where a 3% weight loss occurs within the temperature range matching the last exotherm of the DSC thermogram. In other words, the exotherm at 260°C may come from further curing of oxirane and the thermal decomposition.

The reaction enthalpy of oxirane polymerization with multiple exotherms and irregular baseline of the thermogram is difficult to measure accurately. The kinetics of this epoxy/BF3-MEA system cannot be analyzed properly by traditional DSC methods. Therefore, the ASTM E 698 method has been adopted to overcome these limitations. The ASTM E 698 method assumes (1) the extent of the reaction at the exotherm peak, α_P, is constant and independent of heating rate, (2) the reaction rate constant obeys the Arrhenius equation [k = A exp($-$Ea/RT)], and (3) the reaction is first order [dα/dt = $k(1-\alpha)$]. This ASTM method requires several DSC scans at different heating rates. Based on the obtained linear relationship between the reciprocal of exotherm peak temperature (T_P) and the logarithm of the heating rate (log β), the Ozawa method[20,21] can be used to calculate the activation energy (Ea) of the system as follows:

$$\mathrm{Ea} \cong -2.19\mathrm{R}[\mathrm{d}\log\beta/\mathrm{d}(1/T_P)]$$

The pre-exponential factor (A) can then be evaluated:

$$\mathrm{A} \cong \beta\mathrm{Ea}^* \exp(\mathrm{Ea}/\mathrm{R}T_P)/\mathrm{R}T_P^2$$

According to the assumption (1) of the ASTM E 698, the extent of reaction at exotherm peak is identical. As shown in Figure 2, the close area (I)

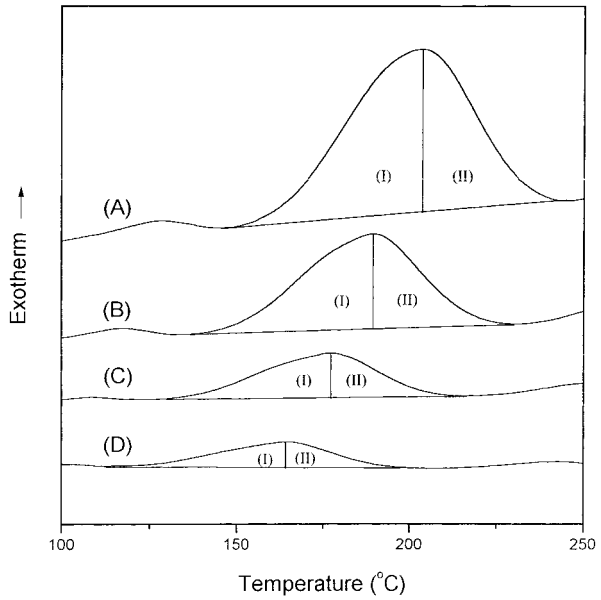

Figure 2. DSC thermogram of DER 331/BF_3-MEA with different heating rates. (A) 20°C /min, ΔH_I = 144.0 J/g; (B) 10°C/min, ΔH_I = 148.6 J/g; (C) 5°C/min, ΔH_I = 140.0 J/g; (D) 2.5°C /min, ΔH_I = 140.3 J/g.

is observed for different heating rates (from 140.0 J/g to 148.6 J/g). In this study, area (I) is divided into four equal parts as area (a), (b), (c), and (d) as shown in Figure 3. Therefore, the corresponding temperatures T_a, T_b, T_c, and T_d all can be fitted to

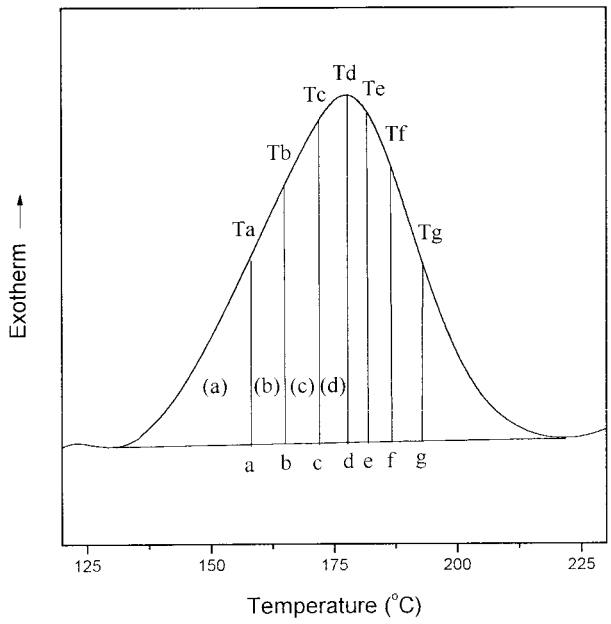

Figure 3. Diagram of separated areas of the DER 332/BF_3-MEA system at heating rate of 10°C/min.

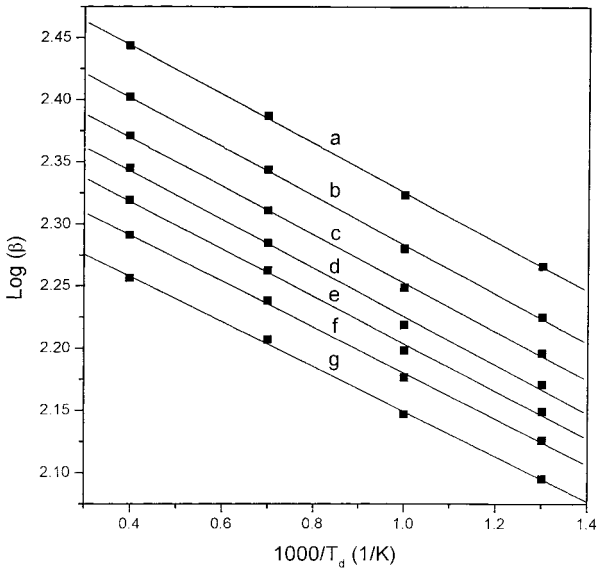

Figure 4. Plots of logβ vs. 1,000/T_d for the DER 332/BF_3-MEA system. The solid lines are regression lines.

the assumption (1) of the ASTM E 698. The complementary area (II) is also divided into four equal parts and temperatures of T_e, T_f, and T_g can also be analyzed by this method. Figure 4 shows plots of the logarithm of heating rate versus the reciprocal of the analyzed temperature for the DER 332/BF_3-MEA system resulting in high linearity. This means that the ASTM E 698 is applicable in this system, and the calculated kinetic parameters of this system should be valid and are summarized in Table II. The activation energies, Eas, deviate within 10% (92–105 kJ/mol) while the pre-exponential factors (A) vary more significantly. Therefore, the apparent reaction rate constants also vary substantially.

Modification of the Data

The pre-exponential factor (A) generally reflects the collision frequency of the reactant molecules. During early stages of reaction, the monomer concentration is expected to be higher and thus the pre-exponential factor is also higher. The temperature effect of different curing procedures is expressed by the Arrhenius equation exp(−Ea/kT). Higher temperature induces higher motion speed of molecules, and thus increases the possibility of collision and reaction rate. The temperature effect can be quantified by a modification factor (m), which obeys the Arrhenius equation exp(−Ea/kT). Since the exotherm peak (point d in Fig. 3)

Table II. Kinetic Parameters Analyzed by the Exotherm Profile of the DER 332/BF_3-MEA System[a]

Analyzed Point	d log(β)/d(1/T_X) X = a, b, . . . g	Activation Energy Ea (kJ/mol)	Pre-Exponential Factor A	Apparent Reaction Rate k at 130°C (1/min)
a	−5054.3	92.10	1.15×10^{11}	0.134
b	−5161.5	93.98	1.22×10^{11}	0.081
c	−5241.2	95.43	1.31×10^{11}	0.057
d	−5380.0	97.96	2.00×10^{11}	0.041
e	−5457.6	99.37	2.25×10^{11}	0.030
f	−5619.1	102.31	3.66×10^{11}	0.020
g	−5751.4	104.72	4.57×10^{11}	0.012

[a] $Ea \cong -2.19R[d \log \beta/d(1/T_X)]$
$A \cong \beta Ea^* \exp(Ea/RT_X)/RT_X^2$
$k = A^* \exp(-Ea/RT_R)$ where $T_R = 130$°C.

shows the highest reaction efficiency, the modification factor (m) can be set as unity. Below this temperature (points a, b, or c), the factor is less than 1. That means slower molecular motion at lower temperature and thus lowers the reaction rate. Above the exotherm peak temperature (point e, f, or g), the factor m is greater than 1, implying higher vibration speed and greater possibility of collision of the reaction. The factor m can be expressed as follows:

$$m = \frac{\exp(-E_a/kT_x)}{\exp(-E_a/kT_d)} = \exp\left(\frac{E_a}{k}\left(\frac{1}{T_d} - \frac{1}{T_x}\right)\right)$$

where E_a = 97.98 kJ/mol (average value of this study) $T_x = T_a, T_b, T_c, T_e, T_f$, and T_g.

Table III lists the calculated factor m and other modified data of the system. The modified reaction rate constant is now fairly close before gelation, an indication that the reaction indeed follows the first order reaction model during early stages of the reaction. The modified reaction rate constant decreases gradually after exotherm peak because the diffusion control begins to dominate the reaction rate.

AM Mechanism

Our previous study[22] using IR and GPC had identified the major component of DER 331 and DER 332 epoxy resin as DGEBA. However, the DER 331 contains substantially higher content of hydroxyl and α-glycol (Table I). The kinetic parameters analyzed by the exotherm peak temperatures of these two epoxy resins are listed in Table IV. The DER 331/BF_3-MEA system shows lower activation energy, pre-exponential factor, and reaction rate constant than

Table III. Modified Kinetic Parameters of the DER 332/BF_3-MEA System[a]

Analyzed Point	Apparent Reaction Rate k at 130°C (1/min)	Modification Factor m	Modified Apparent Reaction Rate Const. k at 130°C (1/min)
a	0.134	0.3386	0.045
b	0.081	0.5456	0.044
c	0.057	0.7597	0.043
d	0.041	1	0.041
e	0.030	1.2891	0.039
f	0.020	1.7316	0.035
g	0.012	2.5466	0.031

[a] $m = \dfrac{\exp(-E_a/kT_x)}{\exp(-E_a/kT_d)} = \exp\left(\dfrac{E_a}{k}\left(\dfrac{1}{T_d} - \dfrac{1}{T_x}\right)\right)$
where Ea = 97.98 kJ/mol (average value of this study).

Table IV. Activation Energy, Pre-Exponential Factor, and Apparent Reaction Rate Constant of This Study[a]

Materials	Items/Unit		
	Activation Energy Ea (kJ/mol)	Pre-Exponential Factor A (1/min)	Apparent Reaction Rate k at 130°C (1/min)
DER 331/BF_3-MEA	95.60	5.74×10^{10}	0.024
DER 332/BF_3-MEA	97.96	2.00×10^{11}	0.041

[a] Analysis based on exotherm peak temperature, T_d.

the corresponding DER 332/BF_3-MEA system. The variations of these observed kinetic parameters can be explained from the cationic polymerization mechanism of oxirane. Penczek et al.[15,16] proposed that the DER 331/BF_3-MEA system follows both ACE and activated monomer (AM) mechanisms as below.

AM Initiation

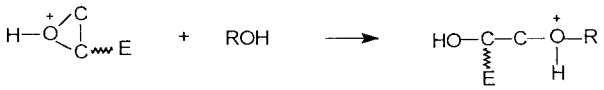

AM Propagation

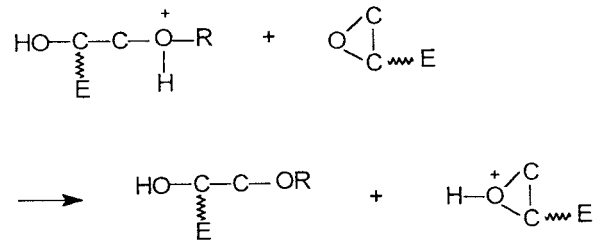

AM Re-Initiation

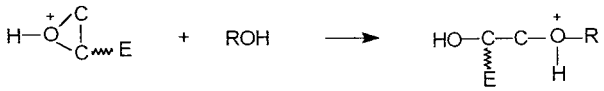

The higher nucleophilicity of a hydroxyl group than an oxirane makes the AM mechanism more favorable than the ACE initiation.[23,24] Therefore, the activation energy Ea of the DER 331/BF_3-MEA system is lower than that of the DER 332/BF_3-MEA system as would be expected. However, the re-initiation and propagation rate of the AM mechanism are slower than the propagation rate of the ACE mechanism because these hydroxyl groups are able to act as a transfer agent to retard the reaction during polymerization.[24] By taking these competition reactions into account, the apparent reaction rate decreases with the presence of hydroxyl groups.

Effect of Hydroxyl Group

Based on above description, the ACE mechanism follows the first order reaction while the AM mechanism does not. Figure 5 shows the plots of logβ versus 1,000/T_d for the DER 332/EG/BF_3-MEA system. When 0.7 phr of the ethylene glycol is added into the system [curve (B)], the slope of the system is indeed slightly lower than the DER 332/BF_3-MEA system due to the appearance of AM mechanism. When a stoichiometric amount of the ethylene glycol (1.8 phr) is added [curve (C)],

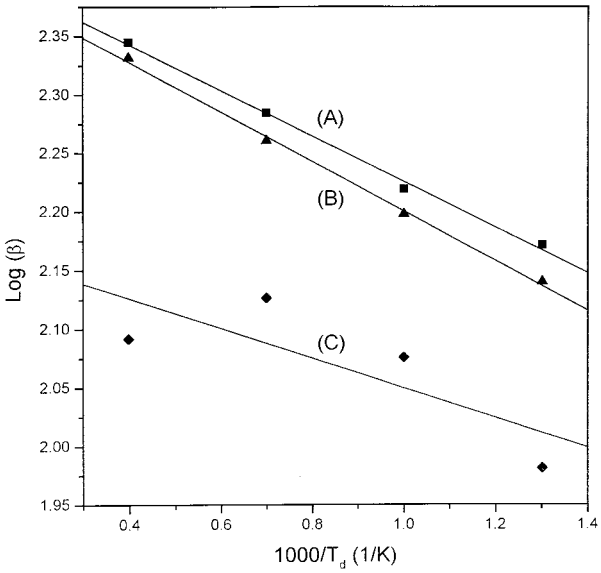

Figure 5. Plots of log β vs. 100/ T_d for the DER 332/BF_3-MEA system. The solid lines are regression lines. (A) DER 332/BF_3-MEA; (B) DER 332/EG(0.7phr)/BF_3-MEA; (C): DER 332/EG(stoichiometric)/BF_3-MEA.

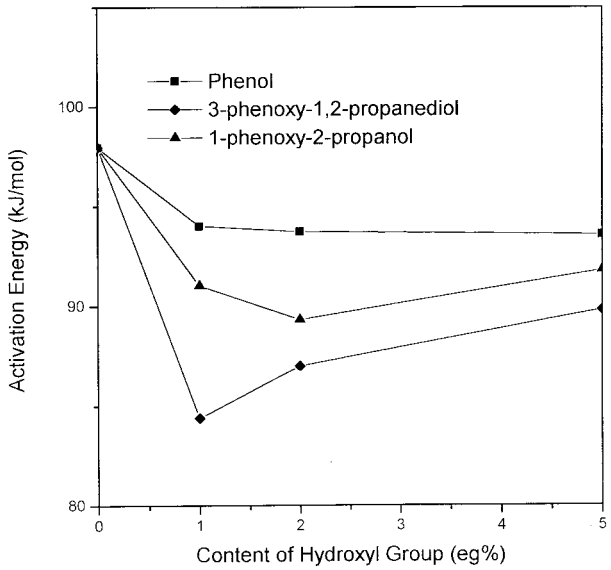

Figure 6. Activation energy Ea (kJ/mol) of the DER 332/hydroxyl group/BF_3-MEA system with different contents of hydroxyl groups.

the AM mechanism becomes dominant and the ACE mechanism is supressed. As the results of the dominant AM mechanism, the system shows poor regression on the plot of logβ versus 1,000/T_d diagram.

In order to compare the effect of different hydroxyl group in DER 331, both 1-phenoxy-2-propanol and 3-phenoxy-1,2-propanediol are used to simulate the presence of secondary alcohol and α-glycol of the DER 331 monomer. Figure 6 shows the effect of hydroxyl group on the activation energy of DER 332/BF_3-MEA system. The presence of 3-phenoxy-1,2-propanediol results in the lower activation energy than that from the 1-phenoxy-2-propanol. The 1°-alcohol structure of 3-phenoxy-1,2-propanediol has stronger nucleophilicity than 1-phenoxy-2-propanol (2°-alcohol only). Therefore, the α-glycol structure in DER 331 resin is mainly responsible for lowering the activation energy to induce the AM mechanism.

Figure 6 also shows less effect of phenol in lowering the activation energy. This can be explained by the fact that the aromatic structure of phenol weakens the nucleophilicity, and results in less change in activation energy.

Another interesting trend shown in Figure 6 is that a higher hydroxyl content (above 1% eq.) actually results in higher activation energy. Since the hydroxyl group can also act as the chain transfer agent, this results in retarding the propagation process and higher activation energy.

Figure 7 shows the activation energies of DER 331/BF_3-MEA, DER 332/BF_3-MEA, and DER 332/BF_3-MEA systems containing 1% eq. content of hydroxyl group during curing. The activation energies from all these systems increase with the progress of reaction. Relative to the DER 332/BF_3-MEA system, the Eas of those systems containing hydroxyl groups (including the DER 331/BF_3-MEA system) increase slower after gelation (processes e, f ,and g). During the diffusion control region, the AM mechanism provides more active sites (hydroxyl group and active oxirane group) than that of the ACE mechanism (active oxirane group only).

Comparison between DER 331/BF_3-MEA and DER 332/BF_3-MEA System

The kinetic results of ASTM E 698 are verified by the DSC, GPC, and FT-IR analysis. Put the DER 331/BF_3-MEA mixture in a 130°C oven, and take a sample every 5 min until the gelation. The only difference in the DER 332/BF_3-MEA system is that the time interval for taking a sample is 4 min. These samples are analyzed by DSC and GPC to measuring the residual monomer ratio and molecular weight. This study also uses a FT-IR to detect the change of oxirane group. The time interval to take a spectrum is the same as above, the only difference is that a heater and a temperature controller are used to maintain the temper-

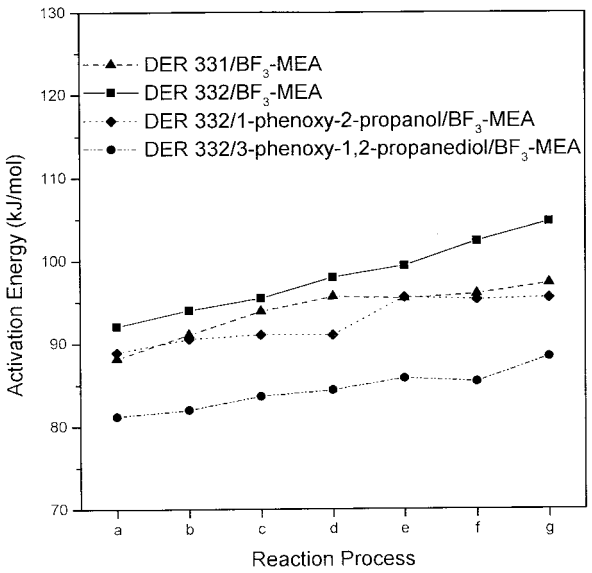

Figure 7. Activation energy Ea (kJ/mol) of the DER 332/hydroxyl group/BF_3-MEA system at different reaction stages.

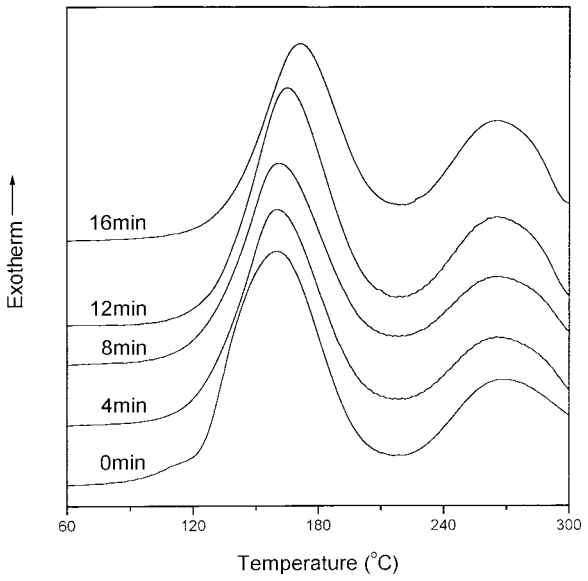

Figure 8. Thermograms of 130°C cured DER 332/BF_3-MEA system at different curing times.

ature of the salt disk, thus there is no need for sampling in this experiment.

Figure 8 shows the thermogram plot of 130°C cured DER 332/BF_3-MEA system at different curing times. The extent of reaction can be obtained by calculating the ratio of the remaining exotherm to the original exotherm. The smaller exotherm near 260°C is ignored in this study for the

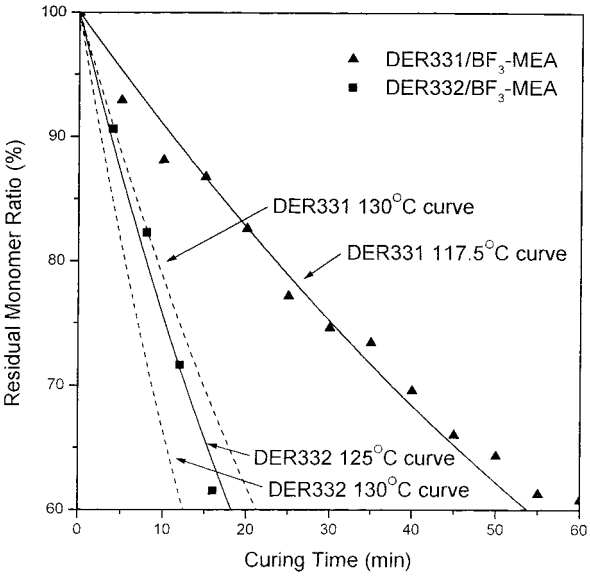

Figure 9. Correlation between the experimental residual monomer ratio (%) at 130°C and the ASTM E 698 theoretically predicted curves.

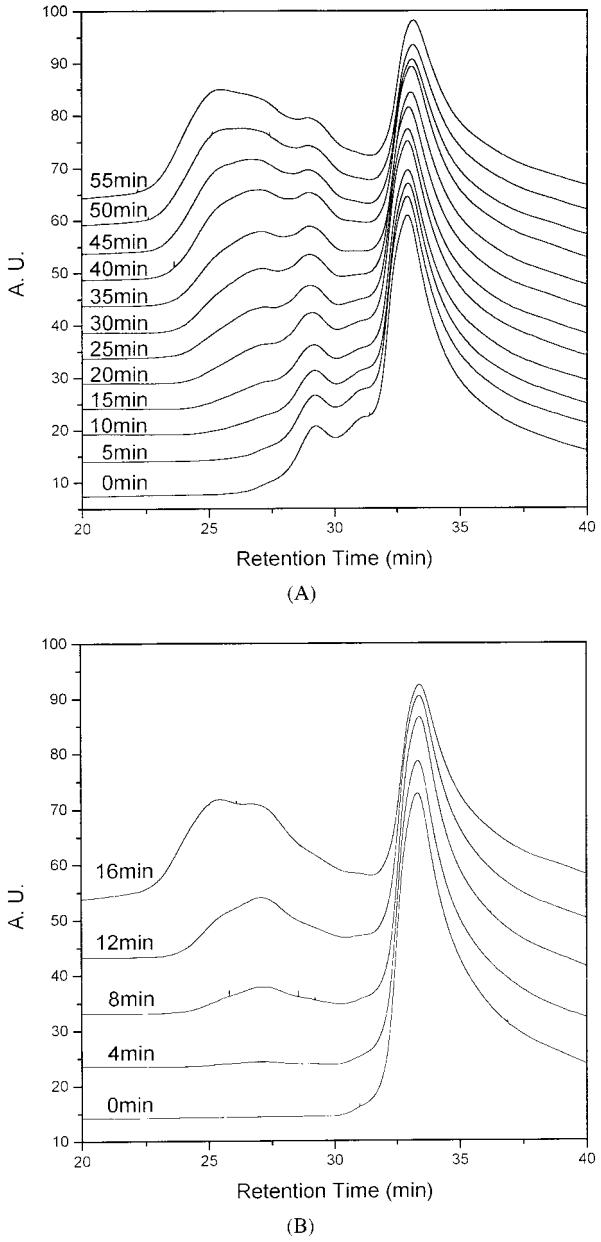

Figure 10. GPC diagrams of the 130°C cured (A) DER 331/BF_3-MEA system, and (B) the DER 332/BF_3-MEA system at different curing times

appearance of degradation reaction. Figure 9 compares the residual monomer ratio at 130°C by experiment and by the thermodynamical simulation based on ASTM E 698. The simulation curve of 125°C fits well with experiment data on the DER 332/BF_3-MEA system. The 5°C deviation can be attributed to the sampling procedure from the temperature-controlled oven and causes the actual temperature to be lower than the set temperature. On the other hand, the deviation of the

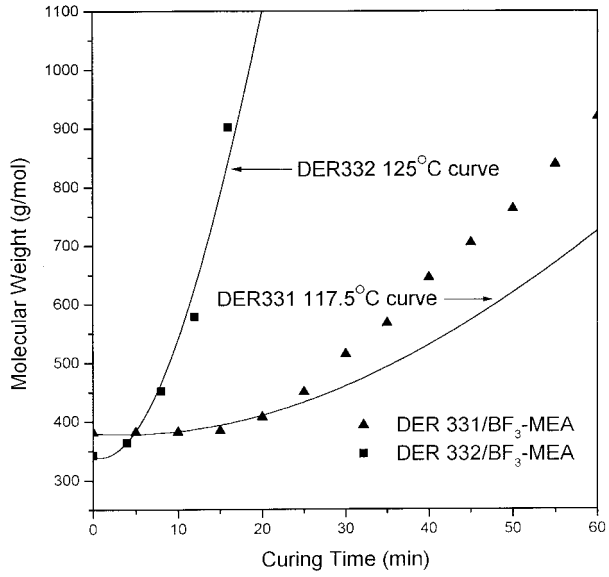

Figure 11. Molecular weight (g/mol) vs. reaction time (min) of 130°C cured DER 331/BF_3-MEA and DER 332/BF_3-MEA systems.

DER 331/BF_3-MEA system is higher than 10°C, implying that the first order reaction model cannot describe the behavior of the DER 331/BF_3-MEA system adequately.

Figure 10(A) and (B) show the GPC diagram of 130°C cured DER 331/BF_3-MEA and DER 332/BF_3-MEA systems at different curing times. The main peak at retention time of 33 min corresponds to the epoxy monomer (n = 0), while the smaller peak at retention time of 29 min in Figure 10(A) is attributed to the epoxy dimer (n = 1) of DER 331. A small peak between them (retention time of 31 min) is the α-glycol containing DGEBA. There is only a peak at 33 min in Figure 10(B), implying that the quantity of other minor components in this DER 332 is insignificant. The molecular weights of these specimens are obtained by calibrating with pure epoxy monomer (n = 0, M.W. = 340 g/mol), dimer (n = 1, M.W. = 608 g/mol) and trimer (n = 2, M.W. = 876 g/mol).

Figure 11 shows the plots of molecular weight (M_w) versus the reaction time (min) of this study. The solid lines in Figure 11 are the theoretically predicted M_w of the system based on the assumption that the polymerization occurs only on the activated chains and molecular weight of each activated chain is identical, as follows:

$$M_W = \frac{\sum NM^2}{\sum NM} = \frac{N_m M_m^2 + N_P M_P^2}{N_m M_m + N_P M_P}$$

where

N_m : mole of residual monomer
N_P : mole of polymer (same mole as BF_3-MEA)
M_m : molecular weight of monomer (380 g/mol and 340 g/mol for DER 331 and DER 332, respectively)
M_P : molecular weight of polymer, which can be calculated by averaging the consumed monomer (measured by DSC) on each polymer chain, as follows:

$$M_P = \frac{N_{m0}\alpha M_m}{N_P}$$

where

N_{m0} : mole of initial epoxy monomer
α : extent of reaction ($= 1 - e^{-kt}$).

Thus, the M_w can be deduced by following:

$$M_W = M_m e^{-kt} + \frac{N_{m0} M_m}{N_P}(1 - e^{-kt})^2$$

The same temperature deviation can be observed in this experiment (5°C for DER 332/BF_3-MEA and 12.5°C for DER 331/BF_3-MEA), which is attributed to the same reason. The larger deviation at higher molecular weight can be attributed to the locally gelation caused by higher degree of polymerization.

The FT-IR can also be used to follow the polymerization process. The 915 cm^{-1} peak corresponds to the epoxide group, and the integrate value of the peak is viewed as the monomer content. Since this peak will not disappear completely after the end of the reaction, the area of this peak is modified by minus the ultimately area. The residual monomer ratio is then obtained by dividing the area of 915 cm^{-1} peak to the original one. Figure 12 shows the plot of residual monomer ratio versus curing time of the study, and the solid lines are the simulation curves based on the ASTM E 698. The DER 332/BF_3-MEA system shows good simulation to 130°C theoretically simulation curve and the deviation for the DER 331/BF_3-MEA system is also smaller (10°C), which is due to the better temperature control of this experiment. Both systems show good correlation before gelation (20 and 60 min for the DER 332/BF_3-MEA and the DER 331/BF_3-MEA system, respectively). The deviation after

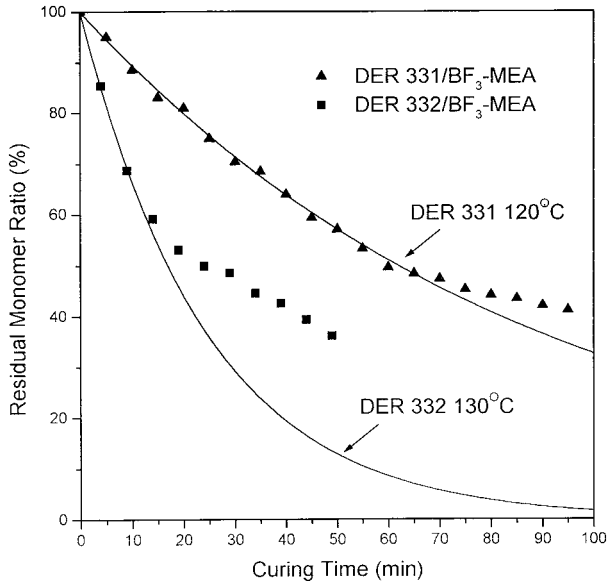

Figure 12. Residual monomer ratio (%) vs. reaction time (min) at 130°C under FT-IR 915cm^{-1} peak measurement.

gelation is attributed to the diffusion control of both systems.

To sum up, the simulation curve based on ASTM E 698 correlates adequately with the results of FT-IR, and the same deviation can be observed with the analyses of DSC and GPC. The better simulation is obtained in the DER 332/BF_3-MEA system because the ACE curing mechanism follows the first order reaction.

The simulation of GPC and FT-IR analyses can only be applied adequately before the system reaches the gel point; after that, the T_g is used to characterize the molecular structure. Figure 13 shows the T_g versus postcure time at 200°C of this study. Experiments were carried out by placing the sample into a 130°C oven for 60 min, and then raising the temperature to 200°C to postcure. The postcure was maintained in vacuum to minimize possible degradation induced by oxidation. Although the DER 332/BF_3-MEA system reacts faster before the gelation than the DER 331/BF_3-MEA system, however, the latter system shows higher T_g after 30 min of postcure. This result confirms that the hydroxyl groups of the DER 331/BF_3-MEA system provide additional reactive sites to react with the remaining epoxy monomer, thus a more condense matrix can be obtained than that of the DER 332/BF_3-MEA system. After 5 h postcure, T_gs of both systems reach 177°C.

CONCLUSIONS

According to the ASTM E 698 analysis, the DER 332/BF_3-MEA system follows the first order active chain end (ACE) reaction mechanism. The pre-exponential factor is higher at the beginning of the reaction because of higher monomer concentration. A correction factor based on Arrhenius equation is adopted into the system, and the apparent reaction rate becomes fairly close after such modification during early stages of the reaction, which agrees with the assumption of first order reaction. The DER 331/BF_3-MEA system follows both the ACE and the activated monomer (AM) mechanisms due to the presence of hydroxyl groups from both α-glycol and 2°-alcohol of the DER 331 epoxy resin. The α-glycol is more effective on inducing AM mechanisms than the 2°-alcohol. That means that the α-glycol structure of the DER 331 resin is mainly responsible for inducing the AM mechanism. The hydroxyl group can also act as a chain transfer agent, thus the activation energy increases gradually with increasing content of the hydroxyl group. The reaction rate of the DER 332/BF_3-MEA system is higher than the DER 331/BF_3-MEA system. Only the DER 332/BF_3-MEA system can be simulated adequately by the first order reaction model before gelation. The FT-IR analysis shows better simulation for the better temperature control of salt disk, while the data of DSC and GPC shows

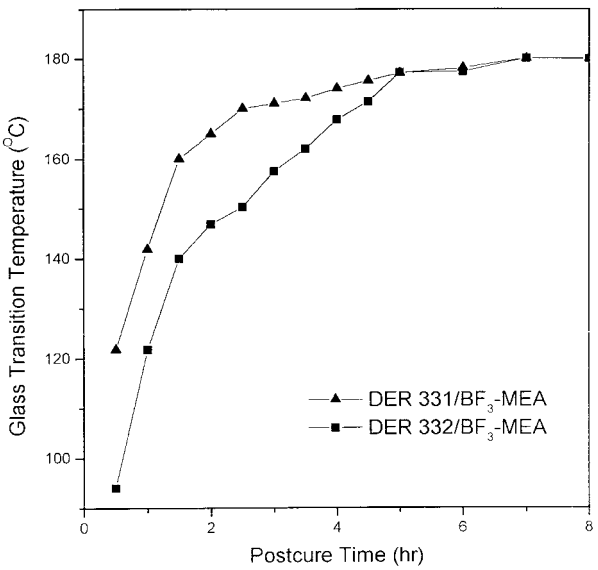

Figure 13. T_g (°C) vs. postcure time (hr) of 200°C cured DER 331/BF_3-MEA and DER 332/BF_3-MEA systems.

5°C deviation for opening the 130°C oven and taking a sample every 4 min. The DER 331/BF_3-MEA system results in higher T_g after 200°C postcure because the hydroxyl group can also act as reactive sites to react with residual epoxy monomers.

This research is financially supported by the National Science Council, Taiwan, Republic of China, under contract NSC 87-2216-E-009-007. We also thank the Epolab Chemical Co. of Taiwan for materials donation.

REFERENCES AND NOTES

1. Senen, P. A.; Arturo, L. Q.; Mercedes, P. P.; Montserrat, V.; Pilar, P. J Polym Sci Poly Chem Ed 1998, 36, 1001.
2. Chandra, R.; Soni, R. K Polym Int 1993, 31, 239.
3. Chiao, L. Macromolecules 1990, 23, 1286.
4. Hsieh, T. H.; Su, A. C. J Appl Polym Sci 1990, 41, 1271.
5. Grillet, A. C.; Galy, J.; Pascault, J. P.; Bardin, I. Polymer 1989, 30, 2094.
6. Spacek, V.; Pouchly, J.; Biros, J. Eur Polym J 1987, 23, 5, 377.
7. Barton, J. M. J Polym Comm 1980, 21, 603.
8. R. D.; Patel, R. G.; Patel, and V. S. Patel, British Polym. J., 1987, 19, 37.
9. Woo, E. M.; Seferis, J. C. J Appl Polym Sci 1990, 40, 1237.
10. Heise, M. S.; Martin, G. C. J Appl Polym Sci 1990, 39, 721.
11. Ghaemy, M. Eur Polym J 1998, 34, 1151.
12. Wendlandt, W. W. Thermal Analysis vol. 1, Ch. 5; New York: Wiley, 1986.
13. ASTM E 698-79.
14. Tackie, M.; Martin, G. C. J Appl Ploym Sci 1993, 48, 793.
15. Penczek, S.; Kubisa, P.; Szymanski, R. Makromol Chem Macromol Symp 1986, 3, 203.
16. Penczek, S.; Kubisa, P.; Szymanski, R. Makromol Chem Macromol Symp 1986, 6, 201.
17. Smith, R. E.; Larsen, F. N.; Long, C. L. J Appl Polym Sci 1984, 29, 3697.
18. Smith, R. E.; Smith, C. H. J Appl Polym Sci 1986, 31, 929.
19. Chen, C. S.; Pearce, E. M. J Appl Polym Sci 1989, 37, 1105.
20. Ozawa, T. J. Therm Anal 1970, 2, 301.
21. Ozawa, T. J. Therm Anal 1970, 9, 369.
22. Li, M. S.; Ma, C. C. M.; Lin, M. L.; Chang, F. C. Polymer 1997, 38, 19, 4903.
23. Hammond, J. M.; Hooper, J. F., Robertson, W. G. P. J Polym Sci A, Polym Chem 1971, 19, 265.
24. Bouillon, N.; Pascault, J. P.; Tighzert, L. Makromol Chem 1990, 191, 1417.